High Spectral Efficiency for Long-haul Optical Links: Time-Frequency Packing vs High-order Constellations

Giulio Colavolpe[(1)] and Tommaso Foggi[(2)]

[(1)] *University of Parma, Dipartimento di Ingegneria dell'Informazione, Parco Area delle Scienze 181/A, I-43124 Parma, Italy*
[(2)] *CNIT, University of Parma, Parco Area delle Scienze 181/A, I-43124 Parma, Italy, tommaso.foggi@nemo.unipr.it*

Abstract. We investigate the time-frequency packing technique on long-haul optical links in order to increase the spectral efficiency. This solution is compared to high-order formats at equal bit or baud rate, demonstrating that higher spectral efficiency can be more effectively reached.

Introduction

The huge data traffic increase on optical networks is leading the research to more sophisticated transmission techniques[1], able to overcome the limits of present-day simple but inefficient systems. The most relevant linear impairments, e.g., group velocity (GVD) and polarization mode dispersion (PMD), have been successfully compensated for with the adoption of coherent detection, that enables the effective equalization of the received signal. However, limitations due to technology and required transmit power, entailing nonlinear (NL) effects, impose to increase the capacity through multi-carrier transmission[2]. The technique proposed in this paper represents a method of efficiently bind up sub-channels, thus allowing a higher spectral efficiency (SE).

The traditional orthogonal signaling paradigm employed in communications ensures no intersymbol (ISI) or inter-carrier interference (ICI), so that, for example, in an optical system with proper pulse shaping, filtering, impairment compensation, and limited NL effects, even a symbol-by-symbol detector attains almost-optimal performance[3]. Multi-carrier systems based on this paradigm are, e.g., orthogonal frequency division multiplexing (OFDM)[4], or Nyquist wavelength division multiplexing (WDM)[5]. In these systems SE can be improved only by employing high-order modulation formats, more sensitive to NL effects and crosstalk. Instead, an alternative is represented by time-frequency packing (TFP)[6,7], which exploits low-order constellations such as quaternary phase shift keying (QPSK), but reducing the spacing between adjacent pulses in time domain through narrow filtering, and at the same time packing the sub-channels closer in the frequency domain. The ISI and ICI intentionally introduced is then managed with the adoption of a proper constrained-complexity detector. SE can be improved by a proper combination of pulse shaping, coding design, linear filtering[8]. Low-order constellations are also known to be more resilient to NL effects, and enable simpler synchronization. The computation of the SE is performed in this paper through a simulation-based method[9], also accounting for NL effects.

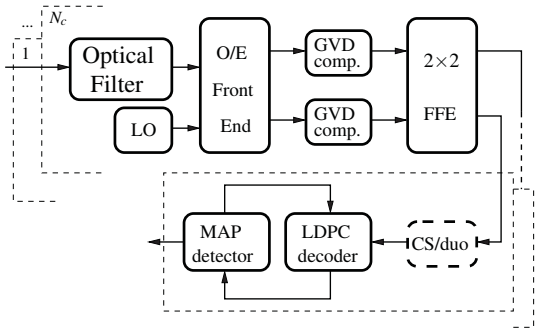

Figure 1. Schematic of the receiver. N_c: number of channels. LO: local oscillator. 2x2 FFE: two-dimensional feedforward equalizer. CS/duo: channel shortener (only for QPSK) or duobinary filtering. MAP: maximum a posteriori. LDPC: low-density parity-check.

Spectral Efficiency Optimization

In the considered scenario, a variable number of equally-spaced polarization-multiplexed sub-carriers are linearly modulated with the same shaping pulse and transmitted over an additive white Gaussian noise (AWGN) channel. The orthogonality paradigm is violated optimizing the frequency spacing F between two adjacent carriers and, theoretically, the symbol time T. However, due to nonlinear Mach-Zehnder (MZ) modulators, signals with support larger than T cannot be generated. Thus, a signal "stretching" is obtained through narrow optical filtering, and our degrees of

freedom become F and the bandwidth B of the (4th-order Gaussian) optical filter at the MZ output. We compared TFP-QPSK with Nyquist-WDM[5] employing 16/64/256-QAM constellations, and duobinary-shaping 16-QAM[10]. OFDM systems were left out because of their practical drawbacks and minor efficiency in optical long-haul systems, as shown in [11].

To compute the SE, it is first necessary to compute the information rate (IR). This is done under a constraint on the complexity of the employed maximum a posteriori (MAP) receivers, assuming parallel independent detectors, one per carrier and per polarization. The information rate (IR) was computed taking into account only a portion of the actual channel memory, defining a proper *auxiliary channel*[9] for which the considered low-complexity receiver is optimal. The computed IR thus represents an achievable lower bound of the IR of the actual channel, when the receivers used for the computation are employed, according to mismatched detection[9]. The achievable SE is thus $\eta = \frac{1}{FT}\mathrm{IR}$ [b/s/Hz]. The proposed technique aims at finding the optimal values of F and B (same at transmit and receive side for TFP) for each signal-to-noise (SNR) value, i.e., we compute $\eta_{\mathrm{M}} = \max_{F,B>0} \eta(F,B)$. Actually, there exist a few regions of SNR where optimal F and B have the same value. For a fair comparison in terms of SE, we define the SNR as the ratio P/N between the signal power and the noise power (in the considered bandwidth). Denoting by K the number of carriers, P/N can as written as $\frac{P}{N} = \lim_{K\to\infty} \frac{KP_C}{N_0((K-1)F+B)} = \frac{P_C}{N_0 F}$, where P_C is the power for each carrier and $N_0/2$ is the two-sided power spectral density of the amplified spontaneous emission (ASE) noise per polarization as if the channel were linear. P_C is independent of the bandwidth B. The given SNR definition is independent of the transmit waveform and its parameters.

For Nyquist-WDM systems, we also optimized the frequency spacing and filter bandwidths, but under the constraint that the spacing is not lower than the Nyquist bandwidth, i.e., 1/T (otherwise we fall in the domain of the TFP technique) and, under this condition, the channel memory is at most limited to one interfering symbol. The memory with TFP can be, instead, very large. We apply a channel shortening (CS) technique[8], which provides an excellent performance by properly filtering the received signal before adopting a reduced-state detector.

Numerical Results

We assume perfect synchronization as we are interested in the evaluation of achievable SE. The SE has been computed for the central channel. However, since we assume a high number of carriers, results do not depend on the considered one. RZ pulses with duty cycle 50% (or NRZ in case of Nyquist-WDM system as in [5]) are employed, and optical transmit filter with 3-dB bandwidth B and receive filter with 3-dB bandwidth B_R, both 4th-order Gaussian, two fixed-tap one-dimensional equalizers (to compensate for GVD) and a two-dimensional (2-D) decision-directed (DD) adaptive feedforward equalizer (FFE) with 25 taps, also used to complete (along with the optical filter) the implementation of the matched filter[3] (i.e., the FFE taps are updated using the MF output as target response, so that the equalizer does not remove the ISI induced by narrow filtering). In the case of systems employing receiver-side duobinary shaping, a further digital filter is present to perform the required shaping[10]. The output is provided to the MAP symbol detectors which iteratively exchange information with the decoders for a maximum of 50 iterations. The system model is reported in Fig. 1. We simulated an existing uncompensated link of standard single-mode fiber (SMF), whose spans are described in Table 1. The fiber dispersion is 16.63 ps/nm/km, the PMD parameter is 0.1 ps/$\sqrt{\text{km}}$, the attenuation is 0.23 dB/km, the nonlinear index γ is equal to 1.3 $\mathrm{W}^{-1}\mathrm{km}^{-1}$, and the noise figure of all amplifiers is equal to 6 dB.

We first considered a systems with 8 140-Gbit/s subchannels, whose baud rate changes for each format. Fig. 2 shows the achievable SE η_{M} for the described systems, where for QAM we used $F = B$ (as mentioned, we imposed the constraint $F \geq 1/T$). The optimized values corresponding to the peak of the η_{M} curves are: $B = 1/T$ and $B_R = 0.7/T$ for 16-QAM, $B = 1.1/T$ and $B_R = 0.85/T$ for 64-QAM, and $B = 1.25/T$ and $B_R = 0.9/T$ for 256-QAM ($B_R < B$ and not $B = B_R$ because we have $F = B$ and the constraint $F \geq 1/T$, and thus in this case is more convenient to reduce B_R with respect to B). At the receiver, the MAP detector memory is $L_r = 2$ for 16-QAM ($L_r = 1$ by definition for the duobinary shaping) and a memory $L_r = 1$ for 64/256-QAM. In the case of TFP, F and B have been optimized for each value of P/N, and it is $B_R = B$. For the Nyquist-WDM system we used $B = 1.1/T$ and $B_R = 1/T$ as suggested in [5] whereas, for receiver-side duobinary shaping we used $B = B_R = 1/T$ as in [10]. The Shannon Limit in the absence of nonlinearities is also shown for comparison. It can be observed that the TFP-QPSK outperforms the other systems. These information-theoretic

Table 1. SMF lengths for each span in the simulated optical link. .

span #	1	2	3	4	5	6	7	8	9	10	11	12	13	14	15
SMF (km)	70.8	75.5	55.1	52.1	40.1	67.	53.2	50	80.3	79.1	53.6	75.1	90.3	54.2	99.4

results can be approached by using proper coding schemes. As an example, we simulated a TFP-QPSK system using $B = 0.36/T$, $F = 0.43/T$, and employing a rate-4/5 low-density parity-check (LDPC) code having codewords of 64800 bits. Assuming a reference for the bit-error rate (BER) of 10^{-7}, the performance of this system has been also reported in Fig. 2 with a diamond. It may be observed that, despite the lack of an optimization in the code design (we used a good code for the linear channel), we have a loss of less than 1 b/s/Hz from the theoretical results, obtaining a SE of 7.5 b/s/Hz. We would like to mention that on this link an experimental field trial demonstration has been also conducted, reaching a SE of more than 5 b/s/Hz despite the constraint to use (poorly performing) 1st-order Gaussian filters, not flexible and penalizing frequency grids, neighbouring commercial traffic, and hurried system optimizations. Fig. 3 reports results of the same modulation formats and optimizations, but with data rate fixed to 50 Gbaud/s and the number of sub-channels set in order to fill approximately a 200 GHz bandwidth (i.e., we simulated 10 sub-channels for TFP-QPSK, 4 sub-channels for 16/64-QAM, and 3 for 256-QAM). Again, TFP-QPSK outperforms all considered M-QAM formats. Although in both simulated scenarios, in principle, 256-QAM with polarization multiplexing could ideally achieve a SE value up to 16 b/s/Hz, it would be reached, in the linear regime, only for higher values of P/N, whereas the optimum launch power corresponds to an SNR value which privileges TFP-QPSK.

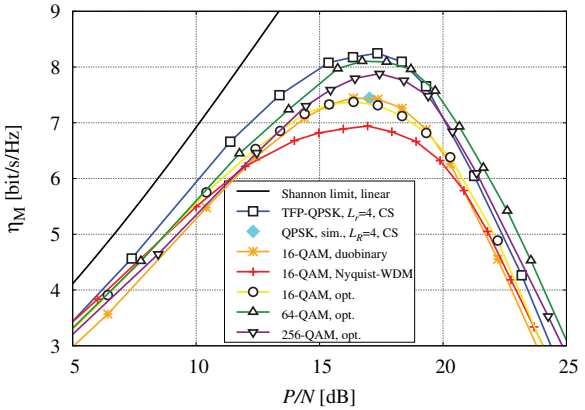

Figure 2. Achievable SE vs. P/N of TFP-QPSK and 16/64/256-QAM with eight 140-Gbit/s subchannels.

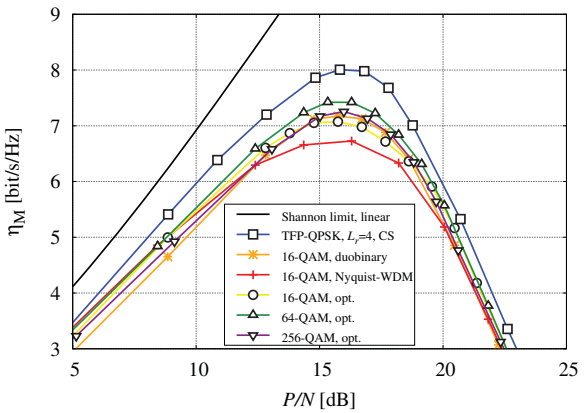

Figure 3. Achievable SE vs. P/N of TFP-QPSK and 16/64/256-QAM with 10/4/4/3 50-Gbaud/s subchannels over 200 GHz bandwidth.

Conclusions

The proposed TFP technique showed to be the most promising solution compared to higher-order modulation formats over a realistic long-haul optical systems. Results show that, when NL effects are present, the spectral efficiency cannot be trivially increased by increasing the modulation order.

Acknowledgements

This work was supported in part by Ericsson and by the Italian Ministero dell'Istruzione, dell'Università e della Ricerca (MIUR) under the FIRB project Coherent Terabit Optical Networks (COTONE).

References

[1] S. Bigo, *Proc. OFC '12*, OTh3A.1 (2012).
[2] S. L. Jansen, *Proc. OFC'12*, OTh1B.1 (2012).
[3] G. Colavolpe *et al.*, *J. Lightwave Technol.* **27**, pp. 2357-2369 (2009).
[4] J. Zhao *et al.*, *J. Lightwave Technol.* **29**, pp. 278-290 (2011).
[5] G. Bosco *et al.*, *J. Lightwave Technol.* **29**, pp. 53-61 (2011).
[6] A. Barbieri *et al.*, *IEEE Trans. Commun.* **57**, pp. 2951-2959 (2009).
[7] G. Colavolpe *et al.*, *Opt. Express*, **19**, pp. 26600-26609 (2011).
[8] F. Rusek *et al.*, *IEEE Trans. Wireless Commun.* **11**, pp. 810-818 (2012).
[9] D. M. Arnold *et al.*, *IEEE Trans. Inform. Theory* **52**, pp. 3498-3508 (2006).
[10] J. Li *et al.*, *J. Lightwave Technol.* **30**, pp. 1664-1676 (2012).
[11] A. Barbieri *et al.*, *J. Lightwave Technol.* **28**, pp. 2537-2551 (2010).
[12] R. Essiambre *et al.*, *J. Lightwave Technol.* **28**, pp. 662-701 (2010).